

## Solid Electrolyte $\text{Li}_{1.4}\text{Al}_{0.4}\text{Ti}_{1.6}(\text{PO}_4)_3$ as Coating for High Voltage Spinel $\text{LiNi}_{0.5}\text{Mn}_{1.5}\text{O}_4$ Cathode Material

Dan Wu<sup>1</sup>, Wei Li<sup>1,2\*</sup>, O. Tegus<sup>1,2</sup>, Yanchun Yang<sup>1,2</sup>, Xiao Tian<sup>1,2</sup>, Siqin Bator<sup>1,2</sup>

<sup>1</sup> College of Physics and Electronic Information, Inner Mongolia Normal University, Hohhot 010022, China.

<sup>2</sup> Inner Mongolia Key Laboratory for Physics and Chemistry of Functional Materials, Hohhot 010022, China.

\*E-mail: [liweisyn@163.com](mailto:liweisyn@163.com)

Received: 5 August 2019 / Accepted: 1 February 2020 / Published: 10 April 2020

A high voltage spinel lithium manganese oxide  $\text{LiNi}_{0.5}\text{Mn}_{1.5}\text{O}_4$ (LNMO) was coated with solid electrolyte  $\text{Li}_{1.4}\text{Al}_{0.4}\text{Ti}_{1.6}(\text{PO}_4)_3$  by a sol-gel method. The experimental samples were characterized by scanning electron microscopy, transmission electron microscopy, X-ray diffraction, charge-discharge analysis, and electrochemical impedance analysis. The experimental results show that coating improves the cyclic performance of LNMO. The capacity retention ratio of the sample coated with 0.50 wt%  $\text{Li}_{1.4}\text{Al}_{0.4}\text{Ti}_{1.6}(\text{PO}_4)_3$  was 98.1% and 96.1% at temperatures of 25 °C and 55 °C, respectively, after 100 cycles and a 1 C rate. Compared with the research results of a  $\text{TiO}_2$  coating agent,  $\text{Li}_{1.4}\text{Al}_{0.4}\text{Ti}_{1.6}(\text{PO}_4)_3$  can promote the diffusion of lithium ions on the surface of the LNMO electrode, reduce the migratory impedance of lithium ions on the surface of the electrode, and improve the rate capability. In contrast,  $\text{TiO}_2$  increases the transport resistance of the lithium ion on the electrode surface and the rate capability decreases. Under the condition of a 20 C rate, the sample coated with  $\text{Li}_{1.4}\text{Al}_{0.4}\text{Ti}_{1.6}(\text{PO}_4)_3$  exhibits 81.3% of its initial capacity, while the sample coated with  $\text{TiO}_2$  only exhibits 74.5% of its initial capacity.

**Keywords:** Lithium-ion battery, Cathode material, High voltage spinel lithium manganese oxide, Surface coating, Solid electrolyte

### 1. INTRODUCTION

Spinel lithium manganese oxide has a structure with a three-dimensional lithium ion channel. It is expected that the above structure will have good application potential in high power batteries[1]. A 4 V spinel lithium manganese oxide has been commercialized, however, its low specific capacity leads to a low energy density of the lithium-ion battery[2]. A high voltage spinel lithium manganese oxide  $\text{LiNi}_{0.5}\text{Mn}_{1.5}\text{O}_4$  (LNMO) retains the advantages of spinel lithium manganese oxide. At the same time, it can enhance the energy density of the lithium-ion battery to a high voltage of 4.7 V, so it has become

one of the most popular materials in recent years[3]. A pristine LNMO has poor cycle performance. The Mn ions contained in LNMO may dissolve due to its disproportionation reaction with the electrolyte, resulting in deteriorating electrode performance[4]. To further improve cycle stability, some other substances have been considered as coatings on the particle surface of LNMO. These coatings can keep the LNMO active materials away from the electrolyte and inhibit the ability of the electrolyte to corrode the LNMO material. Especially at high temperature, the dissolution of Mn in the electrolyte is accelerated, so the high temperature cycling stability of LNMO will be expected to be strengthened after a surface coating process. Usually, surface coating agents include oxides such as Al<sub>2</sub>O<sub>3</sub>[5,6], ZrO<sub>2</sub>[7], ZnO[8], CuO[9], RuO<sub>2</sub>[10,11], CeO<sub>2</sub>[12], Co<sub>3</sub>O<sub>4</sub>[13] and SiO<sub>2</sub>[14]; binary fluorides such as LaF<sub>3</sub>[15] and AlF<sub>3</sub>[16]; ternary compounds such as LaFeO<sub>3</sub>[17], BiPO<sub>4</sub>[18], Li<sub>2</sub>SiO<sub>3</sub>[19], Li<sub>2</sub>TiO<sub>3</sub>[20], and Li<sub>3</sub>PO<sub>4</sub>[21]; and an organic polymer PAN[22], PPy[23]. These studies have played a role in improving the performance of LNMO but have also produced negative effects of increased surface impedance and decreased rate discharge performance of the material.

A solid-state lithium ion electrolyte has a high lithium ion conductivity. Research using solid electrolytes as surface coating agents has been reported. Deng[24] coated a solid electrolyte Li<sub>7</sub>La<sub>3</sub>Zr<sub>2</sub>O<sub>12</sub> to a 4 V spinel lithium manganese oxide LiMn<sub>1.95</sub>Ni<sub>0.05</sub>O<sub>3.98</sub>F<sub>0.02</sub>. The results show that the above coating can improve the cycle performance and rate performance of 4 V lithium manganese oxide at a temperature of 55 °C. The conductivity of a glass ceramic electrolyte Li<sub>1.4</sub>Al<sub>0.4</sub>Ti<sub>1.6</sub>(PO<sub>4</sub>)<sub>3</sub> with a NASICON structure reaches 10<sup>-3</sup> S cm<sup>-1</sup>[25,26]. Research using Li<sub>1.4</sub>Al<sub>0.4</sub>Ti<sub>1.6</sub>(PO<sub>4</sub>)<sub>3</sub> as a coating agent for surface modification has not been reported. In this paper, a study on the surface coating of LNMO with Li<sub>1.4</sub>Al<sub>0.4</sub>Ti<sub>1.6</sub>(PO<sub>4</sub>)<sub>3</sub> is carried out by using a sol-gel method.

## 2. EXPERIMENTAL

### 2.1. The preparation of samples

#### 2.1.1 The preparation of LNMO by surface coating with Li<sub>1.4</sub>Al<sub>0.4</sub>Ti<sub>1.6</sub>(PO<sub>4</sub>)<sub>3</sub>

A precursor was prepared by a co-precipitation method, and a LNMO sample was prepared by a high temperature solid phase method. The LNMO sample was labeled P-LNMO. Then, LiNO<sub>3</sub> (chemical purity), Al(NO<sub>3</sub>)<sub>3</sub>·9H<sub>2</sub>O (chemical purity), Ti(OC<sub>4</sub>H<sub>9</sub>)<sub>4</sub> (chemical purity), and NH<sub>4</sub>H<sub>2</sub>PO<sub>4</sub> (chemical purity) were used as initial reactants for preparing the Li<sub>1.4</sub>Al<sub>0.4</sub>Ti<sub>1.6</sub>(PO<sub>4</sub>)<sub>3</sub> coating agent. The coating dose is calculated as follows: the weight ratio of the coating agent Li<sub>1.4</sub>Al<sub>0.4</sub>Ti<sub>1.6</sub>(PO<sub>4</sub>)<sub>3</sub> to the coated material P-LNMO is 0.25%, 0.50%, and 1.00%, respectively. Weighting three parts of the initial reactants and according to the above ratio, coating Li<sub>1.4</sub>Al<sub>0.4</sub>Ti<sub>1.6</sub>(PO<sub>4</sub>)<sub>3</sub> on the surface of P-LNMO particles was carried out by a sol-gel method. The coated samples were labeled as C-LNMO1, C-LNMO2, and C-LNMO3 in the above ratio order.

The steps of coating Li<sub>1.4</sub>Al<sub>0.4</sub>Ti<sub>1.6</sub>(PO<sub>4</sub>)<sub>3</sub> on the surface of P-LNMO material by the sol-gel method are as follows:

(1)  $\text{Ti}(\text{OC}_4\text{H}_9)_4$  was added to 50 wt% citric acid (chemical purity) solution and stirred for 4 hours. Citric acid was 4 times the mole number of the total metal elements in the designed  $\text{Li}_{1.4}\text{Al}_{0.4}\text{Ti}_{1.6}(\text{PO}_4)_3$ .

(2)  $\text{LiNO}_3$ ,  $\text{NH}_4\text{H}_2\text{PO}_4$ , and  $\text{Al}(\text{NO}_3)_3 \cdot 9\text{H}_2\text{O}$  were added to the above solution and mixed for 1 hour.

(3) The High-voltage lithium manganese oxide P-LNMO was added to the mixed solution and was stirred for 0.5 hours.

(4) A glycol liquid was added into the above mixed solution, and the mole number of glycol was the same as that for citric acid. The esterification reaction occurred for 4 hours at 80 °C, and then the gel formed. Next, the gel was dried at 150 °C.

(5) After drying, the mixture was placed into a muffle furnace for 6 hours of heat treatment at 800 °C. This was followed by natural cooling with the furnace temperature. Finally, high-voltage lithium manganese oxide samples coated with  $\text{Li}_{1.4}\text{Al}_{0.4}\text{Ti}_{1.6}(\text{PO}_4)_3$  were obtained.

### *2.1.2 The preparation of LNMO coated with $\text{TiO}_2$*

$\text{Ti}(\text{OC}_4\text{H}_9)_4$  was used as the initial reactant. According to the above steps, a high-voltage lithium manganese oxide sample coated with 0.50 wt%  $\text{TiO}_2$  was prepared. This sample was marked C-LNMO4.

The preparation of pure phase  $\text{Li}_{1.4}\text{Al}_{0.4}\text{Ti}_{1.6}(\text{PO}_4)_3$  and  $\text{TiO}_2$  were prepared by the sol-gel method according to the above steps without adding P-LNMO.

### *2.2. Physical property characterization method*

The morphology of the sample was analyzed by using a JSM-5600LV scanning electron microscope(SEM). A Japanese electron field emitted high-resolution transmission electron microscope(TEM, JEM-2100F) was used to analyze the sample surface. The accelerating voltage was 200 kV, the point resolution was 0.19 nm, the line resolution was 0.1 nm, and the STEM resolution was 0.2 nm. The phase identification of the prepared samples was carried out by X-ray diffraction (XRD) using a Multiflex X-ray powder diffractometer with a monochromatic Cu radiation source.

Analysis of Mn loss after cycling: the battery after the cycle test was disassembled in a glove box. The residual electrolyte and negative plate were placed in a beaker, soaked in  $\text{HCl}(1 \text{ mol L}^{-1})$ solution for 24 hours, and then the solution was extracted. The Mn element concentration was measured by a standard operating curve method on an Optima 4300DV ICP-AES instrument produced by PE company in the United States.

### *2.3 Method of electrochemical performance analysis*

#### 1) CR2032 battery assembly

P-LNMO, C-LNMO1, C-LNMO2, C-LNMO3, and C-LNMO4, which prepared by the above experiments, were used as positive electrode materials, and lithium metal was used as a negative

electrode material to make a R2032 button cell.

2 ) Determination of capacity and cycling performance for high voltage spinel lithium manganese oxide

The capacity and cycling performances were tested by a LAND CT-2001A multichannel battery test system which produced by Wuhanjinnuo Electronics Co., LTD. The voltage range of the test was 3.0 V~ 5.0 V, and the test current of the first charge capacity and discharge capacity was 0.2 C( $1\text{C}=148\text{ mA g}^{-1}$ ). The test current used for cyclic performance was 1 C.

3) Alternating current impedance analysis

An electrochemical workstation (CHI660d, Shanghai Chenhua Instrument Co., LTD.) analyzes and tests AC impedance. The AC impedance test conditions were as follows: frequency scanning range of 0.01~100 kHz with an amplitude of 5 mV.

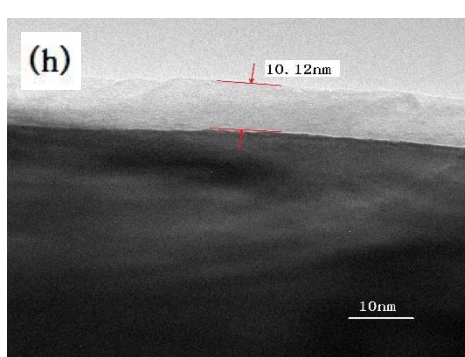
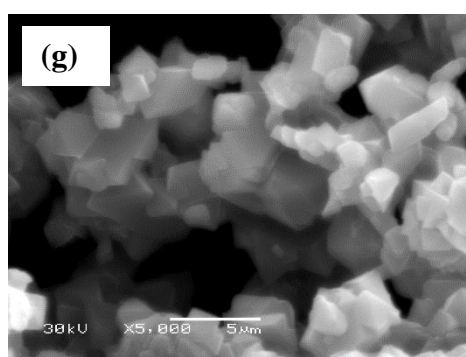
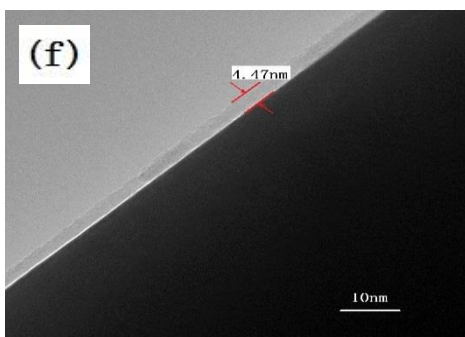
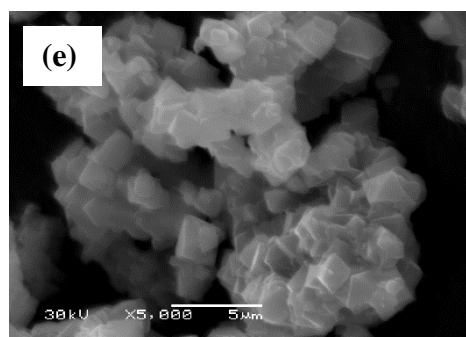
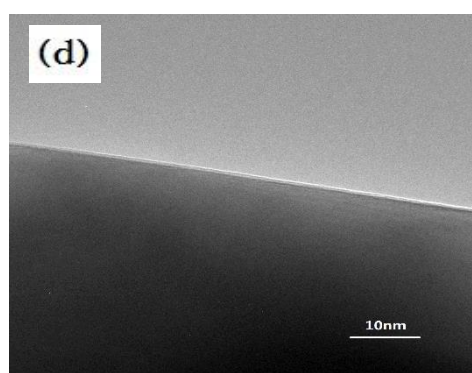
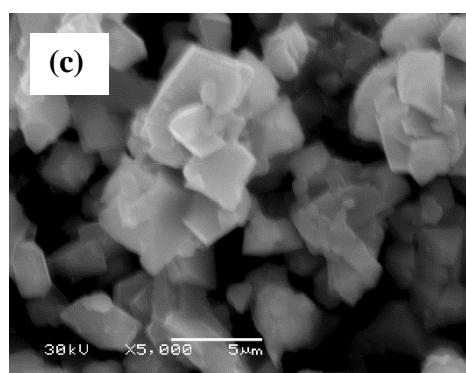
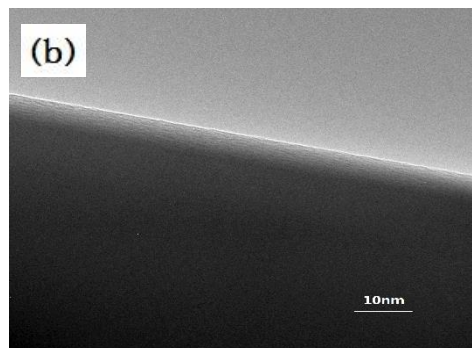
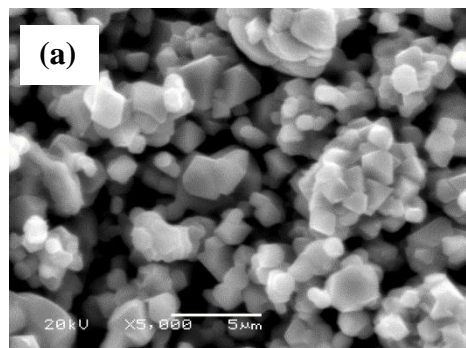
### 3. RESULTS AND DISCUSSION

#### 3.1 Physical and chemical properties of the high voltage lithium manganese oxide

##### 3.1.1 Morphology analysis results of the high voltage lithium manganese oxide before and after coating

Figure 1 shows the SEM and TEM images of the high voltage lithium manganese oxide before and after coating, in which (a), (c), (e), (g) and (i) are the SEM images of P-LNMO, C-LNMO1, C-LNMO2, C-LNMO3, C-LNMO4, respectively, and (b), (d), (f), (h) and (j) are the TEM images, respectively. It can be seen from the SEM images that all the high voltage lithium manganese oxide material samples consist of single octahedral particles. The size of the largest particle does not exceed 5  $\mu\text{m}$ , but some particles stick together. SEM images show that the morphology of the samples has no obvious change before and after coating.

As seen from the transmission electron microscope photos, the uncoated P-LNMO has a flat surface and no other substances observed. The surface of C-LNMO1 coated with 0.25 wt%  $\text{Li}_{1.4}\text{Al}_{0.4}\text{Ti}_{1.6}(\text{PO}_4)_3$  has folds, but it has no obvious stratification. An apparent cladding layer can be seen on the surface of C-LNMO2 coated with 0.50 wt%  $\text{Li}_{1.4}\text{Al}_{0.4}\text{Ti}_{1.6}(\text{PO}_4)_3$ . The thickness of the cladding layer is uniform, and the thickness value is 4.47 nm. The surface coating thickness of C-LNMO3 coated with 1.00 wt%  $\text{Li}_{1.4}\text{Al}_{0.4}\text{Ti}_{1.6}(\text{PO}_4)_3$  increases to 10.12 nm, which indicates that the coating thickness increases with the amount of coating agent. The surface coating thickness of C-LNMO4 coated with 0.50 wt%  $\text{TiO}_2$  is 5.96 nm.



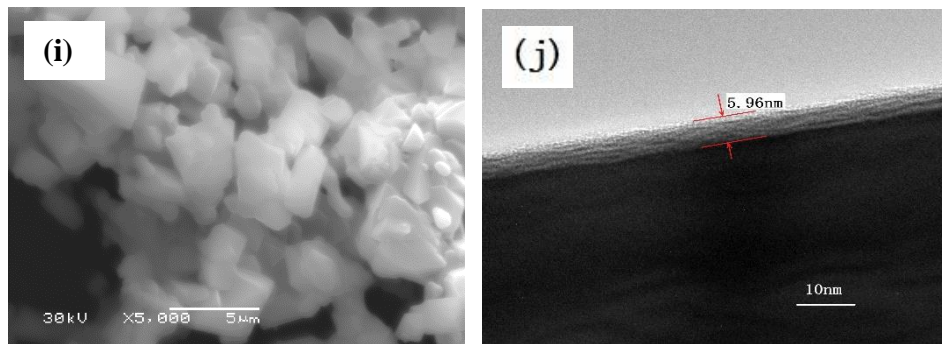


**Figure 1.** SEM images of pristine and coated LNMOs: (a) P-LNMO; (c) C-LNMO1; (e) C-LMNO2; (g) C-LMNO3; and (i) C-LMNO4. TEM images of pristine and coated LNMO: (b) P-LNMO (d) C-LNMO1; (f) C-LMNO2; (h) C-LMNO3; and (j) C-LMNO4.

### 3.1.2 XRD analysis results

To ascertain whether the coating scheme of this experiment is feasible, it is necessary to verify whether the pure phase  $\text{Li}_{1.4}\text{Al}_{0.4}\text{Ti}_{1.6}(\text{PO}_4)_3$  and  $\text{TiO}_2$  can be prepared under the conditions of this experiment. Figure 2 (a) and (b) show the X-ray diffraction pattern of the coating agent  $\text{Li}_{1.4}\text{Al}_{0.4}\text{Ti}_{1.6}(\text{PO}_4)_3$  and  $\text{TiO}_2$  prepared by the sol-gel method. Figure 2 (a) shows that the prepared  $\text{Li}_{1.4}\text{Al}_{0.4}\text{Ti}_{1.6}(\text{PO}_4)_3$  sample shows a typical Na Super Ionic Conductor (NASICON) solid electrolyte structure, which has the same spectra as that of  $\text{Li}_{1.4}\text{Al}_{0.4}\text{Ti}_{1.6}(\text{PO}_4)_3$  prepared by Xu et al.[26]. The results in Figure 2 (b) show that the prepared samples have a typical  $\text{TiO}_2$  structure as verified by the standard card (JCPDS 99-0008)[27] spectrum. Thus, the sol-gel method in this experiment can prepare pure phase  $\text{Li}_{1.4}\text{Al}_{0.4}\text{Ti}_{1.6}(\text{PO}_4)_3$  and  $\text{TiO}_2$  under the necessary conditions (at 800 °C, heat treatment for 6 hours) of the coating process. Furthermore, the experimental scheme of coating  $\text{Li}_{1.4}\text{Al}_{0.4}\text{Ti}_{1.6}(\text{PO}_4)_3$  and  $\text{TiO}_2$  on the surface of lithium manganese oxide with a high voltage by the sol-gel method is feasible.

Figure 2 (c) shows the X-ray diffraction patterns of high voltage lithium manganese oxide samples before and after coating. The diffraction angle ( $2\theta$ ) ranges from 10° to 90°. As shown in the figure, the XRD pattern conforms to a  $\text{Fd}3\text{m}$  structure (JCPDS 35-0782)[28]. Diffraction peaks of other substances are not detected, indicating that the crystal structure of the material did not change after coating with  $\text{Li}_{1.4}\text{Al}_{0.4}\text{Ti}_{1.6}(\text{PO}_4)_3$  and  $\text{TiO}_2$ .

Figure 2 also shows that the diffraction peak intensity of the P-LNMO sample is lower than that of the other samples, which can be caused by the high temperature treatment of the other samples during the coating process. The  $I_{(311)}/I_{(400)}$  ratios of P-LNMO, C-LNMO1, C-LMNO2, C-LMNO3, and C-LMNO4 of the samples are 0.950, 0.949, 0.950, 0.950 and 0.951, respectively. The  $I_{(311)}/I_{(400)}$  ratio reflects the degree of tetragonal distortion from the cubic spinel structure[29]. The  $I_{(311)}/I_{(400)}$  ratios of the sample hardly changed before and after coating, indicating that the coating treatment did not change the atomic arrangement in the material crystal.  $\text{Li}^+$  still occupies the 8a position of the tetrahedron, and no other atoms invade the 8a position to cause a distortion in the crystalline lattice.

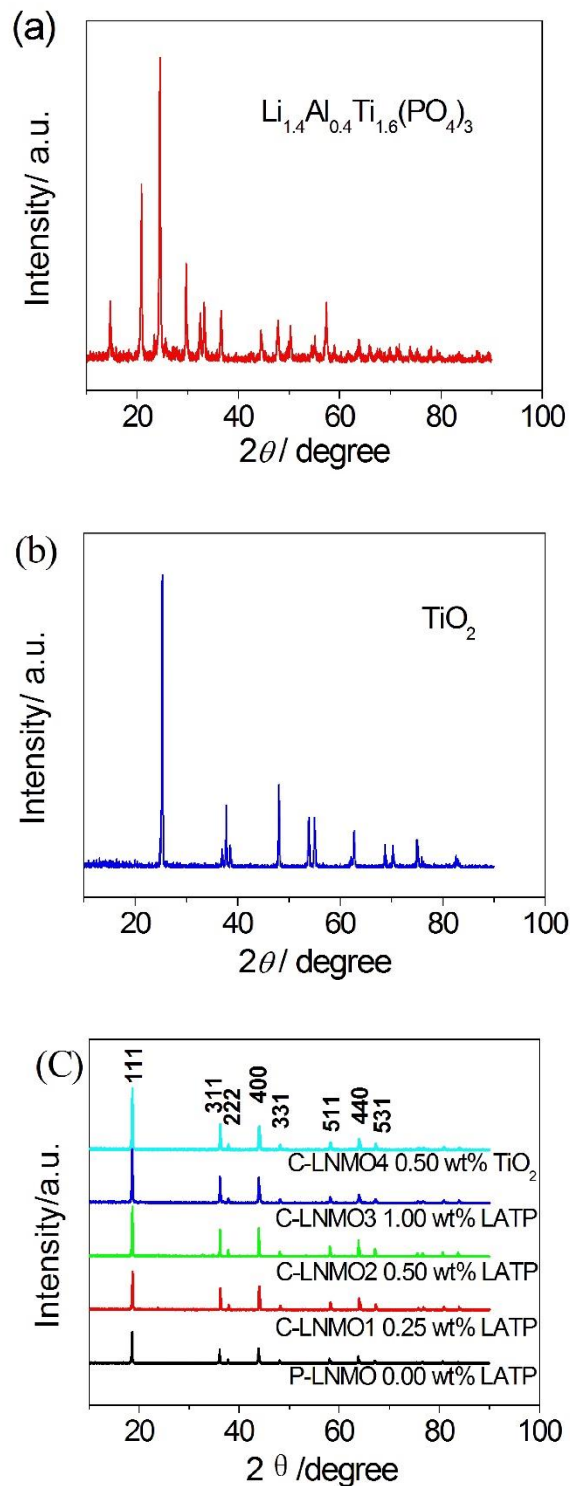


**Figure 2.** XRD patterns of  $\text{Li}_{1.4}\text{Al}_{0.4}\text{Ti}_{1.6}(\text{PO}_4)_3$  (a);  $\text{TiO}_2$  (b); and the pristine and coated LNMOs (c).

### 3.2 Electrochemical properties of the coated high voltage lithium manganese oxide

#### 3.2.1 Characteristic analysis of the charge and discharge performance

Figure 3 shows the first charge and discharge curves of the samples before and after coating. At room temperature, the discharge specific capacities of P-LNMO, C-LNMO1, C-LNMO2, C-LNMO3, and C-LNMO4 samples at 0.2 C were  $135.2 \text{ mAh g}^{-1}$ ,  $133.4 \text{ mAh g}^{-1}$ ,  $132.3 \text{ mAh g}^{-1}$ ,  $130.4 \text{ mAh g}^{-1}$ , and  $131.5 \text{ mAh g}^{-1}$ , respectively. Compared with that of the uncoated sample, the discharge specific capacity of samples coated with  $\text{Li}_{1.4}\text{Al}_{0.4}\text{Ti}_{1.6}(\text{PO}_4)_3$  and  $\text{TiO}_2$  decreased. The extent of the decreased discharge specific capacity increases with an increasing coating amount. The reason for the decrease of discharge specific capacity is that the coating material  $\text{Li}_{1.4}\text{Al}_{0.4}\text{Ti}_{1.6}(\text{PO}_4)_3$  and  $\text{TiO}_2$  do not participate in the electrochemical reaction, but they do occupy a certain mass proportion, so the discharge specific capacity is reduced. The effect of the coating amount of  $\text{Li}_{1.4}\text{Al}_{0.4}\text{Ti}_{1.6}(\text{PO}_4)_3$  on the specific discharge capacity is consistent with that of  $\text{AlF}_3$ [16].

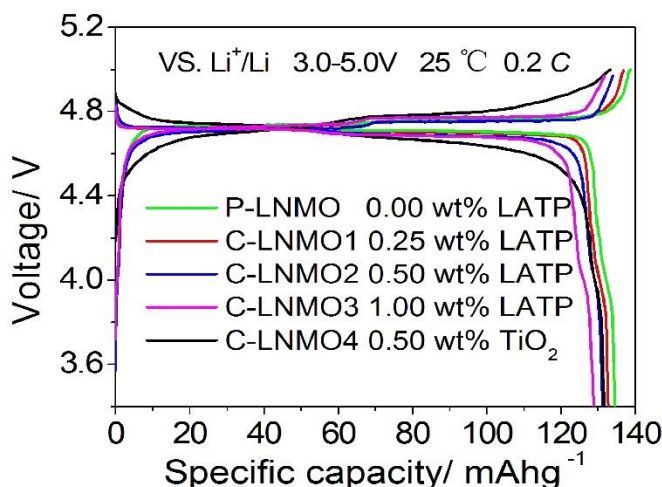


**Figure 3.** Initial charge/discharge curves of pristine and coated LNMOs.

The percentages of the 4.7 V discharge platform capacity to the total discharge capacity are 84.8%, 85.0%, 85.4%, 82.5%, and 64.3%, in the order of P-LNMO, C-LNMO1, C-LNMO2, C-LNMO3, C-LNMO3, and C-LNMO4, respectively. The results show that the C-LNMO2 sample coated with 0.50 wt%  $\text{Li}_{1.4}\text{Al}_{0.4}\text{Ti}_{1.6}(\text{PO}_4)_3$  has the highest platform capacity, while the C-LNMO4 voltage platform coated with 0.50 wt%  $\text{TiO}_2$  evidently decreases. This indicates that the inner resistance of the battery is increased by coating with  $\text{TiO}_2$ .

#### 3.2.2 Cyclic performance at room temperature

Figure 4 is the cyclic performance curve of the high voltage lithium manganese oxide samples before and after coating at a room temperature of 25 °C and a rate of 1 C. The results in Figure 4 show that the surface coating improves the cycling performance of the material at room temperature. For the samples coated with an increasing dose of  $\text{Li}_{1.4}\text{Al}_{0.4}\text{Ti}_{1.6}(\text{PO}_4)_3$ , the retention ratio of recycling capacity increases gradually. The retention ratios of recycling capacity are 95.5%, 96.9%, 98.1%,

97.7%, and 97% after 100 cycles. The pristine sample presents the lowest capacity retention ratio. When the dose of coating agent reaches 1.00 wt%, the retention ratio of circulating capacity does not increase. This indicates that the best effect can be achieved when the dose of coating agent is 0.50 wt%. With an increasing dose of coating agent, the specific capacity of the material decreases, so it is not appropriate to increase the dose of the coating agent. When 0.50 wt%  $\text{TiO}_2$  is used as the coating agent, the cycling performance is also improved; however, the improvement effect is not as good as that with  $\text{Li}_{1.4}\text{Al}_{0.4}\text{Ti}_{1.6}(\text{PO}_4)_3$ . The results of comparing the cycling stability of our sample with those similar structure of LNMO reported in the previous literature are showed in Table 1. The coated LNMO in this work exhibits good capacity retention.

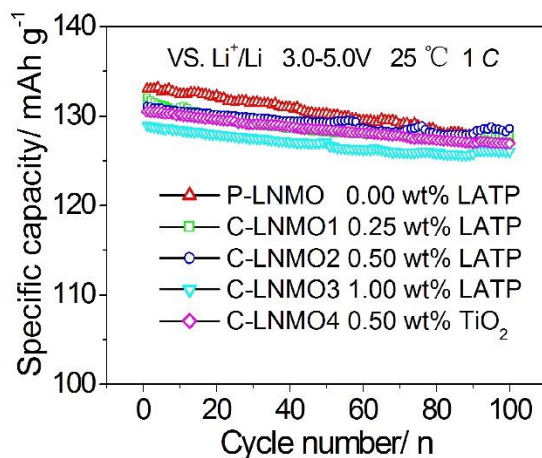


**Figure 4.** Cyclic performance of the pristine and coated LNMOs at room temperature.

### 3.2.3 Cyclic performance at high temperature

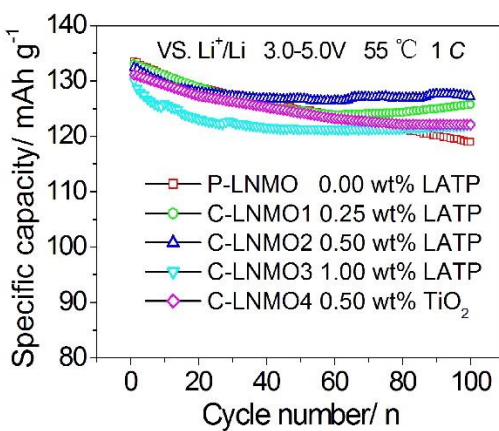


**Figure 5.** Cyclic performance of the pristine and coated LNMOs at high temperature.

Figure 5 shows the cyclic performance curve of high voltage lithium manganese oxide samples before and after coating at a high temperature of 55°C and a rate of 1 C. The results in Figure 5 show that the cyclic properties of the coated samples are also improved at a high temperature. With an increasing dose of coating agent, the cyclic performance improves gradually. The retention ratios of recycling capacity are 89.1%, 94.4%, 96.1%, 93.8%, and 93.1% after 100 cycles. When the dose of

$\text{Li}_{1.4}\text{Al}_{0.4}\text{Ti}_{1.6}(\text{PO}_4)_3$  coating agent is 0.50 wt%, the optimum effect can be achieved. Similarly, when 0.50 wt%  $\text{TiO}_2$  is used as the coating agent, the cycling characteristics at a high temperature are also improved, but the improvement effect is not as good as that with  $\text{Li}_{1.4}\text{Al}_{0.4}\text{Ti}_{1.6}(\text{PO}_4)_3$ .

### 3.2.4 Rate capabilities

The rate performance is one of the most important performance indices of battery power materials. Figure 6 shows the rate performance curve before and after coating. For the samples coated with an increasing dose of  $\text{Li}_{1.4}\text{Al}_{0.4}\text{Ti}_{1.6}(\text{PO}_4)_3$ , the rate performance is improved gradually. The percentage of discharge capacity of 1 C, 5 C, 10 C and 20 C to 0.2 C shows that the capacity gradually increases, and the retention ratio of the circulating capacity also gradually increases. When the dose of coating agent is 0.50 wt%, the percentages of the discharge specific capacity of 1 C, 5 C, 10 C, 20C to 0.2C shows that the discharge specific capacities are 99.3%, 94.5%, 87.3% and 81.3%, respectively; after 20 cycles, the capacity retention ratio is 99.7%, 98.3%, 98.2% and 96.3%, respectively. When the dose of coating agent reaches 1.00 wt%, the retention ratio of circulating capacity is equivalent to that when the dose of coating agent is 0.50 wt%.

When 0.50 wt%  $\text{TiO}_2$  was used as the coating agent, the percentage ratios of 1 C, 5 C, 10 C and 20 C to 0.2 C were 98.0%, 89.5%, 83.5% and 74.5%, respectively; after 20 cycles, the retention rates of circulating capacity were 99.4%, 96.2%, 97.2% and 95.4%, respectively. The discharge characteristics of high-rate discharge decrease obviously. The percentage of discharge specific capacity to 0.2 C of the  $\text{TiO}_2$  at high magnification was lower than that of the samples coated with  $\text{Li}_{1.4}\text{Al}_{0.4}\text{Ti}_{1.6}(\text{PO}_4)_3$  and lower than the uncoated samples. The high magnification cycling characteristic is better than that of the uncoated sample but worse than that of the samples coated with  $\text{Li}_{1.4}\text{Al}_{0.4}\text{Ti}_{1.6}(\text{PO}_4)_3$ . The results of comparing the rate capabilities of our sample with those similar structure of LNMO reported in the previous literature are showed in Table 1. The coated LNMO in this work demonstrates an optimum rate capability.

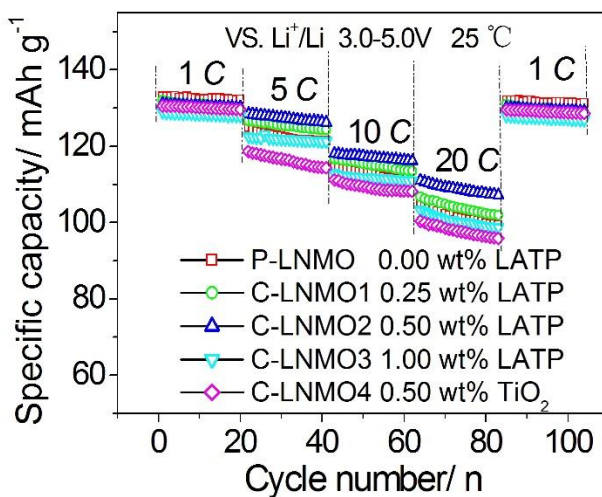


**Figure 6.** Rate performances of the pristine and coated LNMOs.

**Table 1.** Comparison of the electrochemical performance for surface modified LNMO samples reported in literature with this work.

Samples	Capacity retention (%)	Rate performance (mAh g <sup>-1</sup> )	Reference
LNMO/C	64.0@10C, after 500 cycles	112@5C,104@10C	[30]
LNMO/RuO <sub>2</sub>	97.7@0.5C, after 100 cycles	66.1@10C	[10]
LNMO/CuO	95.0@0.5C, after 100 cycles	98.7@10C	[9]
LNMO/TiO <sub>2</sub>	88.0@2C, after 500 cycles	97.6@7C,88.3@10C	[31]
LNMO/PAALi	90.0@0.2C, after 200 cycles	111.4@6C,101.5@12C	[32]
LNMO/PPy	95.0@1C, after 300 cycles	105@2C,85@5C	[23]
LNMO/Co <sub>3</sub> O <sub>4</sub>	96.8@1C, after 300 cycles	116@6C,97.5@10C	[13]
LNMO/LATP	98.1@1C, after 100 cycles	118@10C,111@20C	this work

### 3.2.5 AC impedance analysis

Figure 7 is the EIS diagram of the sample at room temperature. The illustration in the figure is an equivalent circuit to simulate the positive electrode interface, where  $R_s$  represents the bulk impedance of the electrolyte,  $R_{ct}$  represents the migration impedance of lithium ions on the electrode surface,  $C_d$  represents the double-layer capacitance on the surface, and  $Z_w$  represents the material diffusion impedance. The graph of each sample consists of a semicircle and approximately oblique lines. The semicircle at high frequency corresponds to the diffusion of lithium ions in the interface layer between the electrodes and electrolytes, and the oblique line at low frequency corresponds to the diffusion of lithium ions in the bulk phase of the active material[31]. The point of intersection between the semicircle curve and the X-axis on the left can be considered  $R_s$ , while the point of intersection on the right can be considered  $R_{ct}$ .

As shown in the figure, the  $R_s$  values of sample P-LNMO, C-LNMO1, C-LNMO2, C-LNMO3, and C-LNMO4 are between 10 Ω and 30 Ω, and the values are close. While the values of  $R_{ct}$  have a greater difference, they are 122 Ω, 115 Ω, 76 Ω, 79 Ω, and 179 Ω, respectively. Therefore, it is clear that coating with Li<sub>1.4</sub>Al<sub>0.4</sub>Ti<sub>1.6</sub>(PO<sub>4</sub>)<sub>3</sub> reduces  $R_{ct}$  when the amount of Li<sub>1.4</sub>Al<sub>0.4</sub>Ti<sub>1.6</sub>(PO<sub>4</sub>)<sub>3</sub> is 0.50 wt%, and  $R_{ct}$  drops to the lowest value of 76 Ω. When the amount of Li<sub>1.4</sub>Al<sub>0.4</sub>Ti<sub>1.6</sub>(PO<sub>4</sub>)<sub>3</sub> increases to 1.00 wt%,  $R_{ct}$  starts to increase again, so the best dose is 0.50 wt%. When cladding by using 0.50 wt% TiO<sub>2</sub>,  $R_{ct}$  sharply increases to 179 Ω. This shows that titanium dioxide prevents the migration of lithium ions on the surface of the electrode. The results explain why the discharge platform performance reduces for the sample of C-LNMO4 coated with TiO<sub>2</sub> in Figure 3; furthermore, the coating of Li<sub>1.4</sub>Al<sub>0.4</sub>Ti<sub>1.6</sub>(PO<sub>4</sub>)<sub>3</sub> increases the rate performance while the coating of TiO<sub>2</sub> decreases the rate performance as shown in Figure 6. The results of coating with TiO<sub>2</sub> are similar to those of coating with Al<sub>2</sub>O<sub>3</sub>, which increases the battery impedance and weakens the rate capability [6]

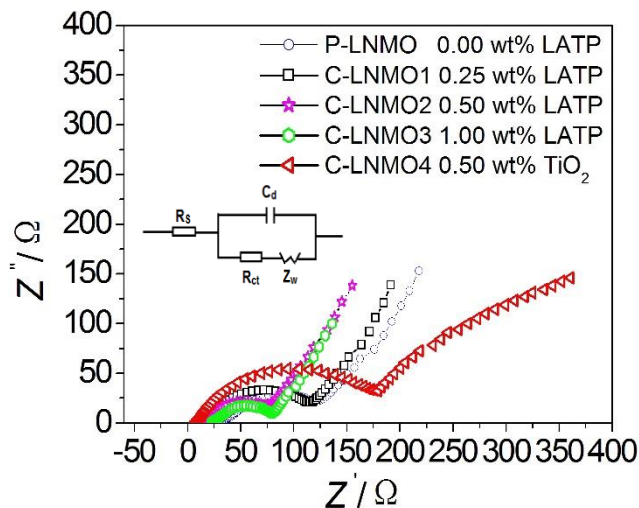


**Figure 7.** The EIS of the pristine and coated LNMOs.

### 3.2.6 Manganese determination during the charging and discharging cycling process

As reported in previous studies[33,34], the primary reason for the cyclic life attenuation of positive electrode materials containing manganese lithium ions is the loss of the manganese ions, which are dissolved in the electrolyte. After the manganese ions dissolve, on the one hand, they move to the negative electrode and damage it during the charging and discharging process; on the other hand, the cathode material suffers structural collapse forming a cationic-deficient spinel phase because of the loss of manganese. The lattice damage leads to the blocking of the Li<sup>+</sup> diffusion channel. These reasons lead to reversible capacity loss and cycle performance degradation. Surface coating is an effective technology to prevent manganese from being dissolved. In this experiment, the total manganese content that dissolves in the electrolyte and moves to the negative electrode after 100 cycles is determined, and the results are shown in Table 2.

The results in Table 2 show that the surface coating can significantly reduce the dissolved amount of manganese whether conducted at a room temperature of 25 °C or at a high temperature of 55 °C. This indicates that the coating can effectively prevent the erosion of cathode materials by an electrolyte. The coating is more effective in preventing manganese from dissolving at high temperature than that at room temperature. For the samples coated with Li<sub>1.4</sub>Al<sub>0.4</sub>Ti<sub>1.6</sub>(PO<sub>4</sub>)<sub>3</sub>, as the coating agent increased, the dissolved amount of manganese decreased gradually. When the coating agent varied from 0.25 wt% to 0.50 wt%, the solubility of manganese showed the greatest decline. When the coating agent increased from 0.50 wt% to 1.00 wt%, the amount of dissolved manganese decreased slightly. This indicates that an appropriate amount of coating agent can achieve the best result. When the dose of coating agent is 0.50 wt%, an intact coating layer can be formed with a coating thickness of 4.47 nm, as shown in Figure 1(f). The coating of this thickness can effectively inhibit the dissolution of manganese atoms. When the amount of coating agent increased again, the decrease in manganese dissolution is very small, so 0.50 wt% is the best dose. The experimental results show that coating with TiO<sub>2</sub> also prevents manganese dissolution.

**Table 2.** Amount of coating agent and concentration of Mn dissolved from LNMO ( $C_{\text{Mn}}$ ) after cycling at different temperatures.

Sample	Coating agent	Amount /wt%	$C_{\text{Mn}}$ at 25°C /mg L <sup>-1</sup>	$C_{\text{Mn}}$ at 55°C /mg L <sup>-1</sup>
P-LNMO		0.00	56	122
C-LNMO1	Li <sub>1.4</sub> Al <sub>0.4</sub> Ti <sub>1.6</sub> (PO <sub>4</sub> ) <sub>3</sub>	0.25	49	116
C-LNMO2	Li <sub>1.4</sub> Al <sub>0.4</sub> Ti <sub>1.6</sub> (PO <sub>4</sub> ) <sub>3</sub>	0.50	33	71
C-LNMO3	Li <sub>1.4</sub> Al <sub>0.4</sub> Ti <sub>1.6</sub> (PO <sub>4</sub> ) <sub>3</sub>	1.00	29	68
C-LNMO4	TiO <sub>2</sub>	0.50	31	66

#### 4. CONCLUSIONS

Using an appropriate amount of Li<sub>1.4</sub>Al<sub>0.4</sub>Ti<sub>1.6</sub>(PO<sub>4</sub>)<sub>3</sub> as a coating agent, a coating layer of uniform thickness can be obtained on the surface of lithium manganese oxide at high voltage by a sol-gel method. The coating decreases the original discharge specific capacity of high voltage lithium manganese oxide. The coating significantly improves the cycling stability of high-voltage lithium manganese oxide, especially the cycling stability at high temperature. The capacity retention ratio of the sample coated with 0.50 wt% Li<sub>1.4</sub>Al<sub>0.4</sub>Ti<sub>1.6</sub>(PO<sub>4</sub>)<sub>3</sub> reaches 98.1% and 96.1% at temperatures of 25 °C and 55 °C, respectively, after 100 cycles and a 1 C rate. Furthermore, 0.50 wt% Li<sub>1.4</sub>Al<sub>0.4</sub>Ti<sub>1.6</sub>(PO<sub>4</sub>)<sub>3</sub> is more effective at improving the stability of high-temperature circulation. The rate capability of high voltage lithium manganese oxide can be significantly improved by being coated with Li<sub>1.4</sub>Al<sub>0.4</sub>Ti<sub>1.6</sub>(PO<sub>4</sub>)<sub>3</sub>. When TiO<sub>2</sub> is used as a coating agent, the rate capability of high voltage lithium manganese oxide decreases. When the coating agent is 0.50 wt%, the sample coated with Li<sub>1.4</sub>Al<sub>0.4</sub>Ti<sub>1.6</sub>(PO<sub>4</sub>)<sub>3</sub> can release 81.3% of a 0.2 C capacity at a 20 C rate, whereas the sample coated with TiO<sub>2</sub> can only release 74.5% of a 0.2 C capacity. Li<sub>1.4</sub>Al<sub>0.4</sub>Ti<sub>1.6</sub>(PO<sub>4</sub>)<sub>3</sub> can reduce the interface impedance, while titanium dioxide increases the interface impedance. Finally, coating effectively prevents the dissolution of manganese after long-term cycling at room temperature and high temperature.

#### ACKNOWLEDGEMENTS

This work was financially supported by the National Natural Science Foundation of China (No. 21865021), the High-level Scientific Research Foundation for the Introduction of Talent of Inner Mongolia Normal University(No. 2018YJRC019) and the Inner Mongolia Normal University graduate students' research & Innovation fund(No. CXJJS19104).

#### References

1. N. Nitta, F.X. Wu, J.T. Lee, G. Yushin, *Materials Today*, 18(2015) 252.
2. G.J. Xu, Z.H. Liu, C.J. Zhang, G.L. Cui, L.Q. Chen, *J. Mater. Chem. A*, 3(2015) 4092.
3. Z. Zhu, D. Zhang, H. Yan, W. Li, L. Qi, *J. Mater. Chem. A*, 1(2013) 5492.
4. N.P.W. Pieczonka, Z.Y. Liu, P. Lu, K.L. Olson, J. Moote, B.R. Powell, J.H. Kim, *J. Phys. Chem.*

- C, 117(2013) 15947.
- 5. J.W. Kim, D.H. Kim, D.Y. Oh, H. Lee, J.H. Kim, J.H. Lee, Y.S. Jung, *J. Power Sources*, 274 (2015) 1254.
  - 6. Y. Wang, Q. Peng, G. Yang, Z. Yang, L.C. Zhang, H. Long, Y.H. Huang, P.X. Lu, *Electrochim. Acta*, 136 (2014) 450.
  - 7. G.H. Lee, I.H. Choi, M.Y. Oh, S.H. Park, K.S. N.V. Aravindan, Y.S. Lee, *Electrochim. Acta*, 194 (2016) 454.
  - 8. J.C. Arrebola, A. Caballero, L. Hernán, J. Morales, *J. Power Sources*, 195 (2010) 4278.
  - 9. X.L. Li, W. Guo, Y.F. Liu, *Electrochim. Acta*, 116 (2014) 278.
  - 10. S.H. Jung, D.H. Kim, P. Brüner, H. Lee, H.J. Hah, S.K. Kim, Y.S. Jung, *Electrochim. Acta*, 232 (2017) 236.
  - 11. Q. Pang, Q. Fu, Y.H. Wang, *Electrochim. Acta*, 152 (2015) 240.
  - 12. T.F. Yi, X. Han, B. Chen, Y.R. Zhu, Y. Xie, *J. Alloys Comp.*, 703 (2017) 103.
  - 13. M.M Deng, Z.F. Tang, Y. Shao, X.D. He, Z.Y. Wen, C.H. Chen, *J. Alloys Comp.*, 762 (2018) 163.
  - 14. Y.K. Fan, J.M. Wang, Z. Tang, W.C. He, J.Q. Zhang, *Electrochim. Acta*, 52 (2007) 3870.
  - 15. Y.P. Li, Q. Zhang, T.H. Xu, D.D. Wang, D. Pan, H.L. Zhao, Y. Bai, *Ceram. Int.*, 44 (2018) 4058.
  - 16. Q. Wu, Y.F. Yin, S.W. Sun, X.P. Zhang, N. Wan, Y. Bai, *Electrochim. Acta*, 158 (2015) 73.
  - 17. J.R. Mou, Y.L. Deng, L.H. He, Q.J. Zheng, N. Jiang, D.M. Lin, *Electrochim. Acta*, 260 (2018) 101.
  - 18. J. Liu, Y.F. Cheng, Q.L. Fan, L.Y. Zhang, L.Y. Liu, X. Ke, N.G. Wang, Z.C. Shi, Z.P. Guo, *Materials Letters*, 214 (2018) 68.
  - 19. Y.L. Deng, L.H. He, J. Ren, Q.J. Zheng, C.G. Xu, D.M. Lin, *Mater. Res. Bull.*, 100 (2018) 333.
  - 20. K. Zhang, P. Li, M. Ma, J.H. Park, *J. Power Sources*, 336 (2016) 307.
  - 21. S. Yubuchi, Y. Ito, T. Matsuyama, A. Hayashi, M. Tatsumisago, *Solid State Ionics*, 285 (2016) 79.
  - 22. W.Q. Lin, J. Wang, R. Zhou, B.H. Wu, J.B. Zhao, *Int. J. Electrochem. Sci.*, 12 (2017) 12047.
  - 23. X.W. Gao, Y.F. Deng, D. Wexler, G.H. Chen, S.L. Chou, H.K. Liu, Z.C. Shi, J.Z. Wang, *J. Mater. Chem.*, 3 (2015) 404.
  - 24. Y.F. Deng, S.X. Zhao, D.H. Hu, C.W. Nan, *J. Solid State Electrochem.*, 18 (2014) 249.
  - 25. S.D. Jackman, R.A. Cutler, *J Power Sources*, 218(2012) 65.
  - 26. X.X. Xu, Z.Y. Wen, J.G. Wu, X.L. Yang, *Solid State Ionics*, 178(2007) 29.
  - 27. R. Wang, J.N. Deng, J. Li, M.Q. Tang, P.Y. Li, Y. Zhang, *Int. J. Electrochem. Sci.*, 15 (2020) 567.
  - 28. Y.S. Li, J. Wang, Z.F. Zhou, Q.R. Yao, Z.M. Wang, H.Y. Zhou, J.Q. Deng, *Int. J. Electrochem. Sci.*, 14 (2019) 2822.
  - 29. J.B. Jiang, K. Du, Y.B. Cao, Z.D. Peng, G.R. Hu, J.G. Duan, *J. Alloys Comp.*, 577 (2013) 138.
  - 30. H. Wang, Z. Shi, J. Li, S. Yang, *J. Power Sources*, 288 (2015) 206.
  - 31. S. Tao, F.J. Kong, C.Q. Wu, X.Z. Su, T. Xiang, S.M. Chen, H.H. Hou , L. Zhang, Y. Fang, Z.C. Wang, W.S. Chu, B. Qian, L. Song, *J. Alloys Compd.*, 705 (2017) 413.
  - 32. Q.T. Zhang, J.T. Mei, X.M. Wang, *Electrochim. Acta*, 143 (2014) 265.
  - 33. J.C. Arrebola, A. Caballero, L. Hernán, J. Morales, *J. Power Sources*, 195(2010)4278.
  - 34. J.H. Cho, J.H. Park, M.H. Lee, H.K. Song, S.Y. Lee, *Energy Environ. Sci.*, 5 (2012) 7124.